

Realization of High Efficiency Green Phosphorescent Top-emitting Organic Light-emitting Diodes by Employing Ultrathin Non-doped Emissive Layer

Xindong Shi, Jing Wang, Jun Liu, Saijun Huang, Xinkai Wu, Jiangang Lu, Chaoping Chen, Yikai Su and Gufeng He*

National Engineering Lab for TFT-LCD Materials and Technologies, Department of Electronic Engineering, Shanghai Jiao Tong University, Shanghai, China

Woo Young Kim

Department of Green Energy & Semiconductor Engineering, Hoseo University, Asan, South Korea

Abstract

Green phosphorescent top-emitting organic light-emitting diodes (TOLEDs) based on a single ultrathin non-doped emissive layer (EML) are investigated for utilizing the cavity standing wave effect to enhance device performance. Furthermore, double ultrathin non-doped EMLs separated by a bi-layer structure is introduced to balance charges and further improve the efficiency.

1. Introduction

Phosphorescent top-emitting organic light-emitting diodes (TOLEDs) are particularly suitable for active matrix displays due to their favorable merits, such as high efficiency, large aperture ratio and high pixel resolution. The emissive layer (EML) structures of phosphorescent OLEDs (PHOLEDs) can be categorized into host-guest doped EML and non-doped EML. Actually, most of highly efficient top-emitting monochrome and white OLEDs have been realized based on host-guest EML structure [1]. But, this approach may suffer from the poor reproducibility for mass production processes since it is difficult to accurately control the deposition rate and dopant concentration during multi-source evaporation process, especially for co-host system. In order to simplify the fabrication process and the device structure, the alternative ultrathin non-doped EML-based OLEDs were introduced and have received an increasing interest. For example, Divayana et al. [2] reported OLEDs with a repeating ultrathin non-doped EML structure (host/guest/host/guest/...), which can avoid co-evaporation and simplify the fabrication process. Nevertheless, the device structures were still complex. Recently, highly efficient and simple monochrome blue, green, orange, and red bottom-emitting OLEDs (BOLEDs) based on ultrathin non-doped EMLs have been reported [3]. The even simpler structure and the high efficiency indicate the feasibility of ultrathin non-doped EML-based OLEDs.

However, surprisingly, there are no prior reports of TOLED based on ultrathin non-doped EML. It is well known that the emission of TOLED is not only determined by the cavity of the device, but also strongly dependent on the position of the emitter layer within the two reflectors. The emissive layer can be positioned either at the maximum (antinode) or the minimum (node) field strength of the standing wave, resulting in enhanced or suppressed emission, respectively [4]. The TOLED based on doped EML with a relatively broad recombination zone may be inferior to utilize cavity standing wave effect, compared with that with very narrow one. It is because a certain fraction of emitting light away from antinode obtains fewer enhancements than those close to antinode, as illustrated in Figure 1 (a) and (b).

On the basis of the above analysis, a green phosphorescent TOLED employing a single ultrathin non-doped EML is proposed

for the first time where we focus on the relative efficiency enhancement ratios between TOLED and BOLED with the same layer structure, whereas EML structures are ultrathin non-doped EML structure and conventional host-guest doped EML structure, respectively. Furthermore, by combining dual ultrathin non-doped EMLs isolated by a bi-layer structure, the device achieves a higher current efficiency of 131.4 cd/A at a luminance of 1000 cd/m² and maintains to 113.3 cd/A at 10,000 cd/m².

2. Experimental

Figure 1 (c) shows the layer structures of the investigated TOLEDs with an optical optimized configuration, in which the device T1 utilizes doped host-guest system as EML while the device T2 is based on an ultrathin non-doped EML.

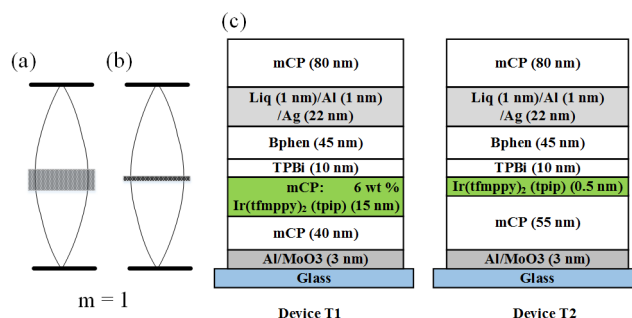


Figure 1 Cavity standing wave patterns for the fundamental mode with a broad (a) and a narrow (b) emission zone; and the layer structures of the investigated TOLEDs (c)

In this study, 1,3-bis(carbazol-9-yl)benzene (mCP) is used as hole transport layer (HTL), which is used as light emitting host as well. For electron transport layer (ETL), we use 4,7-diphenyl-1,10-phenanthroline (Bphen) and 1,3,5-tris(N-phenylbenzimidazole-2-yl)benzene (TPBi), and the latter is also a light emitting host material with predominant electron transport property. The phosphorescent dopant iridium(III)bis(2-(4-trifluoromethylphenyl)pyridine)tetraphenylimidodiphosphinate (Ir(tfmppy)₂(tpip)) [5] is co-evaporated with mCP as emissive layer for doped EML-based devices, while 0.5 nm Ir(tfmppy)₂(tpip) is as EML for ultrathin EML devices. A 3-nm-thick MoO₃ layer and the bi-layer structure 8-hydroxyquinoline lithium (Liq) (1 nm)/aluminum (Al) (1 nm) are utilized as hole and electron injection layer, respectively. To extract additional light from the devices and achieve both appropriate reflectivity and low absorption of the top contact for major emission wavelength of Ir(tfmppy)₂(tpip), an 80-nm-thick mCP deposited

on the silver (Ag) is used as capping layer (CPL). A computer controlled Keithley 2400 and Topcon BM-7A measurement system is used to measure the current density-voltage-luminance characteristics of the devices. The spectral radiant intensity is measured with a calibrated Labsphere CDS 610 spectrometer.

3. Results and discussion

3.1 Single ultrathin EML-based device

To investigate the relative efficiency enhancement between TOLEDs and BOLEDs based on doped EML or non-doped ultrathin EML, two controlled BOLEDs (referred as device B1 and B2) with the similar layer structures were fabricated respectively, except that the reflective Al anode was replaced by transparent indium tin oxide (ITO), and the semi-transparent Ag cathode was replaced by reflective Al electrode.

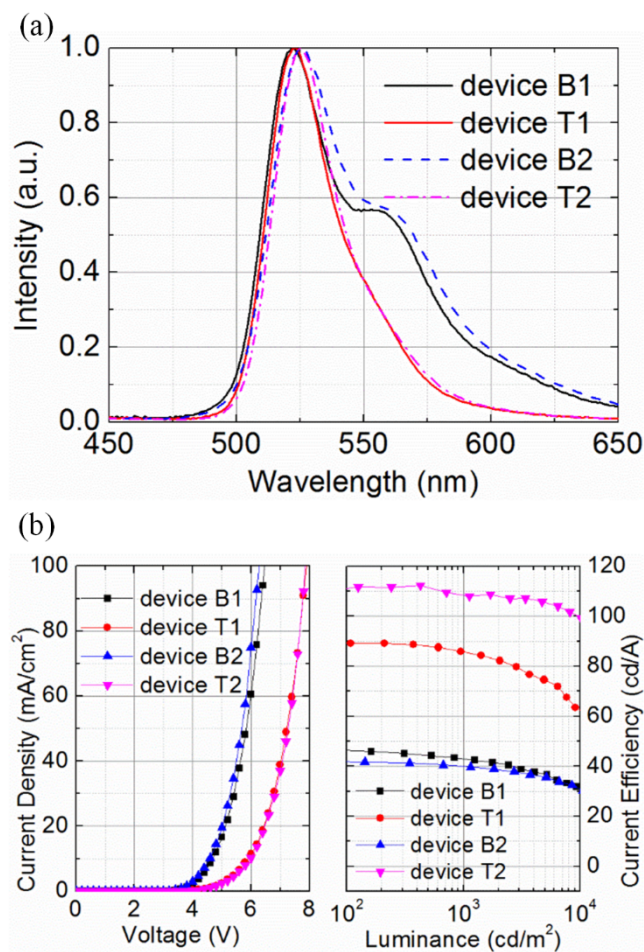


Figure 2 Normalized emission spectra (a), current density-voltage (J-V) and current efficiency-luminance (CE-L) characteristics (b) of device B1, B2, T1 and T2.

Figure 2 (a) shows the normalized electroluminescence (EL) spectra of the four devices. The TOLEDs T1 and T2 exhibit EL peaks at 522 nm and 526 nm, respectively, which are quite close to the EL peaks of corresponding BOLEDs, indicating that the cavity of the TOLED meets the resonant condition. Compared with the device B1 and T1 based on doped EML, there is a slight

red-shift for device B2 and T2 with non-doped ultrathin EML, which may be caused by the presence of an aggregated state.

As shown in Figure 2 (b), the TOLEDs show much lower current densities than BOLEDs, which may be attributed to the poorer hole injection from Al (4.3 eV) anode to mCP (5.9 eV) compared with from ITO (4.7 eV) anode to mCP (5.9 eV) at the presence of a 3-nm-thick MoO₃ hole injection layer. However, the two BOLEDs show comparable electrical properties, so do the two TOLEDs, which suggests that the charge injection and transport in either BOLEDs or TOLEDs are similar for different EML structures. This implies the differences observed in efficiencies of BOLEDs or TOLEDs may be mainly related to the recombination efficiency and microcavity effect. The efficiencies of the four devices are shown in the right part of Figure 2 (b). As it can be seen, device T1 exhibits a current efficiency of 85.7 cd/A at 1000 cd/m², around 2.0 times higher than 43.0 cd/A achieved by device B1. In contrast, the efficiency value of the non-doped ultrathin EML-based device T2 is found to be 108.5 cd/A at 1000 cd/m², up to 2.7 times as high as 40.0 cd/A obtained by non-cavity device B2. It has been well known that the position of the emission layer within the optical microcavity structure has a great influence on the emission intensity of the device. This influence is mainly caused by the standing wave of the electromagnetic field as mentioned above. By restricting the emission zone at the antinode in the ultrathin EML TOLED, a strong enhancement caused by efficient coupling between the emission dipoles and the optical mode can be achieved. On the other hand, relatively poor enhancement is obtained if the active region is broader.

To further investigate the influence of standing wave effect, a set of simulation was conducted by finite-difference time-domain (FDTD) method [6], where the modeled structure is glass/Al (100 nm)/organic layer (110 nm)/Ag (22 nm)/CPL (80 nm) with dipole located at between 45 and 60 nm from the reflective Al electrode, while the cavity length is fixed at 110 nm to meet the resonant condition. To match the random orientation and emission behavior of evaporated small molecules, we set three independent orthogonal dipoles and averaged the light intensities in air. The fraction of the power transmitted into the air is obtained by integrating the far field intensity over all viewing angles, which were calculated by FDTD simulation. The out-coupling efficiency is defined by the ratio of the power transmitted into the air to the total radiated power of a dipole source, as depicted in Figure 3. It can be seen that the out-coupling efficiency increases initially with the increase of the distance between dipole and reflective electrode. After reaching a maximum at around 55 nm, the out-coupling efficiency drops with a further increase of distance, indicating that the location (55 nm) is at the first antinode in this optical cavity. This antinode position is in good agreement with the result calculated by Fabry-Pérot resonance equation, which thus confirmed the accuracy of FDTD simulation [7]. The results of the pure optical out-coupling efficiency simulation reveal two important suggestions. First, if an ultra-narrow emission zone is restricted exactly at the antinode, the microcavity device could achieve the best out-coupling efficiency. Secondly, if a relatively broad emission zone (usually more than 10 nm) is placed near the antinode, the out-coupling efficiency of this device will be averaged, and poorer than that of the device based on an ultra-narrow emission zone located at the antinode.

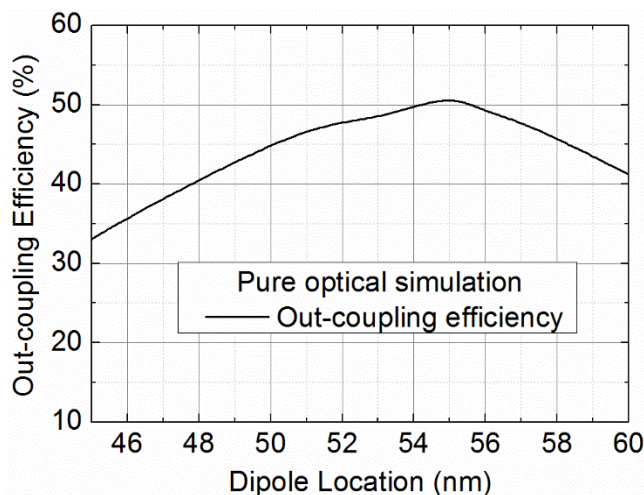


Figure 3 Calculated out-coupling efficiency as a function of different dipole locations at the wavelength of 526 nm

These simulation results are in good agreement with the experimental results mentioned above, where top-emitting device T2 with ultrathin EML has an up to 2.7 times enhancement in current efficiency compared to bottom-emitting device B2, while the device T1 has a normal 2.0 times improvement compared to device B1 with doped EML.

3.2 Dual ultrathin EMLs-based device

The most efficient way to get high recombination efficiency in PHOLEDs is to balance holes and electrons in the EML. A strategy for carrier control is proposed to further improve efficiency by introducing dual ultrathin non-doped EMLs separated by a bi-layer structure. The device structure is Al/MoO₃ (3 nm)/mCP (50 nm)/Ir(tfmppy)₂(tpip) (0.5 nm)/TPBi (2.5 nm)/mCP (2.5 nm)/Ir(tfmppy)₂(tpip) (0.5 nm)/TPBi (10 nm)/Bphen (45 nm)/Liq (1 nm)/Al (1 nm)/Ag (22 nm)/mCP (80 nm), in which a bi-layer structure TPBi (2.5 nm)/mCP (2.5 nm) is used as the separate layers (SLs), as seen in inset of Figure 4 (a). At one point or another, by utilizing this separate layer structure, the thick mCP HTL and the thin 2.5-nm-thick TPBi SL make the first ultrathin Ir(tfmppy)₂(tpip) like “doping” in both mCP and TPBi host, so does the second ultrathin EML. This structure is similar to dual “co-host” systems and is beneficial for carrier balance. The Figure 4 (a) depicts the J-V characteristics, which shows very little difference between devices with a single ultrathin EML and dual ultrathin EMLs, indicating that the separating structure does not affect J-V characteristic of the dual ultrathin EMLs-based device. Nevertheless, it is shown in Figure 4 (b) that the maximum current efficiency of this device reaches 134.0 cd/A at 110 cd/m², and remains as high as 131.4 cd/A at 1000 cd/m² and 113.3 cd/A at 10,000 cd/m², manifesting a current efficiency enhancement of 21.7% compared with a single ultrathin EML-based device at 1000 cd/m². The bi-layer separate layer structure is so thin that the holes and electrons are easy to tunnel through corresponding TPBi and mCP layer, respectively. Therefore, a fraction of excitons will form in the separate layer structure (TPBi (2.5nm)/mCP (2.5nm)), followed by energy transfer to the dopant. On the other hand, a certain fraction of charges (including a portion of carriers tunneling through the separate layers) will transport directly to the dopant sites and be

trapped to form excitons. Furthermore, the excitons will be well confined within the ultrathin EMLs due to the wide band gap and the high triplet energy of mCP and TPBi. It is because the above both mechanisms existed at the same time in the device that the dual ultrathin EMLs surrounded by two hosts of mCP and TPBi can effectively trap tunneled carriers to form excitons and harvest excitons forming in the bi-layer separate layer, as illustrated in inset of Figure 4 (b). In addition, the emission region varies in the range from 50 nm to 55 nm (the distance from reflective electrode), all of which have at least 45% out-coupling efficiencies, as seen in Figure 3.

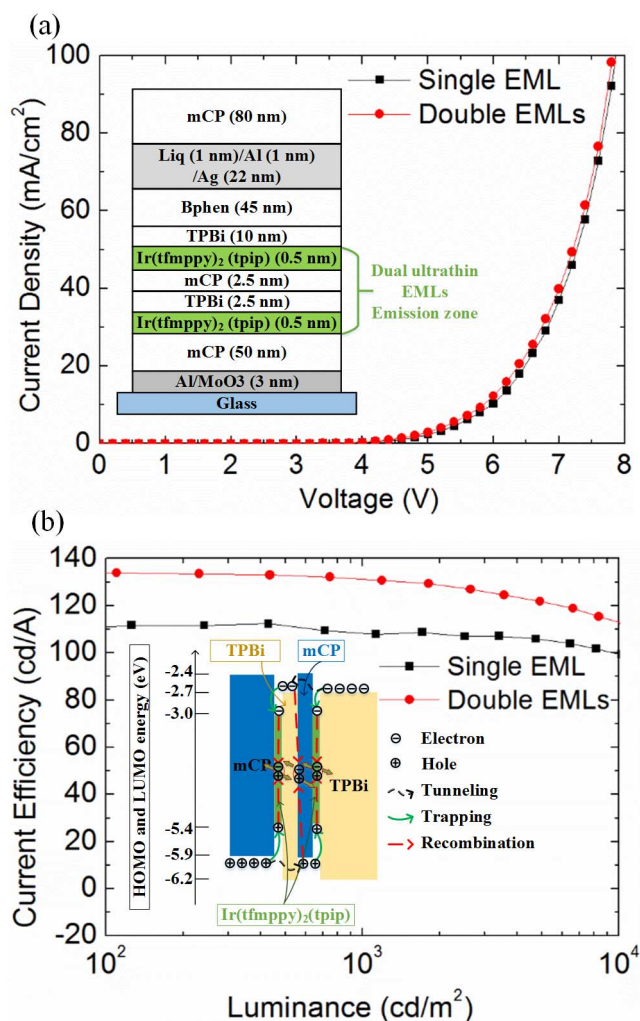


Figure 4 J-V characteristics (a) and inset: dual ultrathin non-doped EMLs-based device structure, and CE-L characteristics (b) and inset: schematic energy diagrams of the device based on the dual ultrathin non-doped EMLs.

4. Summary

It has been demonstrated that an ultrathin non-doped EML-based TOLED satisfying microcavity resonance and standing wave antinode conditions shows a greater relative efficiency enhancement between TOLED and BOLED with the same layer

structure, compared with a conventional doped EML-based TOLED. Dual-ultrathin-EML separated by a bi-layer structure is applied to get more balanced charges and increase recombination efficiency, and a maximum current efficiency of 134.0 cd/A at 110 cd/m² is achieved. This ultrathin non-doped EML-based TOLED is expected to have potential advantages of saving cost, easy control, fabrication and high efficiency for display applications.

5. Acknowledgements

This research work was supported by 973 Program (2013CB328803, 2013CB328804), the National Natural Science Foundation of China (61377030) and the Science and Technology Commission of Shanghai Municipal (12JC1404900).

6. References

- [1] T. Schwab, S. Schubert, M. Thomschke, M. Fröbel, L. Müller-Meskamp, K. Leo, M.C. Gather, "43.3: Inverted Top-Emitting White OLEDs with Improved Optical and Electrical Characteristics," *SID Int. Symp. Digest Tech. Papers*, **44**, 600-603, (2013).
- [2] Y. Divayana, X.W. Sun, "Efficient electrofluorescent organic light-emitting diodes by sequential doping," *Appl. Phys. Lett.*, **90**, 203509-203511 (2007).
- [3] Y. Zhao, J. Chen, D. Ma, "Ultrathin Nondoped Emissive Layers for Efficient and Simple Monochrome and White Organic Light-Emitting Diodes," *ACS Applied Materials & Interfaces*, **5**, 965-971, (2013).
- [4] S. Dirr, S. Wiese, H.-H. Johannes, W. Kowalsky, "Organic Electro- and Photoluminescent Microcavity Devices," *Adv. Mater.*, **10**, 167-171, (1998).
- [5] Y.-C. Zhu, L. Zhou, H.-Y. Li, Q.-L. Xu, M.-Y. Teng, Y.-X. Zheng, J.-L. Zuo, H.-J. Zhang, X.-Z. You, "Highly Efficient Green and Blue-Green Phosphorescent OLEDs Based on Iridium Complexes with the Tetraphenylimidodiphosphate Ligand," *Adv. Mater.*, **23**, 4041-4046, (2011).
- [6] A. Chutinan, K. Ishihara, T. Asano, M. Fujita, S. Noda, "Theoretical analysis on light-extraction efficiency of organic light-emitting diodes using FDTD and mode-expansion methods," *Org. Electron.*, **6**, 3-9, (2005).
- [7] Q. Wang, Z. Deng, D. Ma, "Realization of high efficiency microcavity top-emitting organic light-emitting diodes with highly saturated colors and negligible angular dependence," *Appl. Phys. Lett.*, **94**, 233306, (2009).